

Learning A Task-Specific Deep Architecture For Clustering

Abstract

While deep networks show to be highly effective in extensive applications, few efforts have been spent on studying its potential in clustering. In this paper, we argue that the successful domain expertise of sparse coding in clustering is still valuable, and can be combined with the key ingredients of deep learning. A novel feed-forward architecture, named TAG-LISTA, is constructed from graph-regularized sparse coding. It is then trained with task-specific loss functions from end to end. The inner connections of the proposed network to sparse coding leads to more effective training. Moreover, by introducing auxiliary clustering tasks to the hierarchy of intermediate features, we present DTAG-LISTA and obtain a further performance boost. We demonstrate extensive experiments on several benchmark datasets, under a wide variety of settings. The results verify that the proposed model performs significantly outperforms the generic architectures of the same parameter capacity, and also gains remarkable margins over several state-of-the-art methods.

1. Introduction

Clustering aims to learn the hidden data patterns in an unsupervised way, and group similar patterns among massive data. Generative clustering algorithms model categories in terms of their geometric properties in feature spaces, or as statistical processes of data. Examples include K-means and Gaussian mixture model (GMM) clustering [3], which assume a parametric form of the underlying category distributions. On the other hand, discriminative clustering algorithms search for the boundaries or distinctions between categories. With fewer assumptions being made, these methods are powerful and flexible in practice. Examples include maximum-margin clustering [28], information theoretic clustering [16], and many more.

Most existing clustering algorithms work well when the data dimensionality is low. While partitioning high-dimensional data, their performances are not guaranteed. As suggested by [19], high-dimensional data exhibits dense grouping in low-dimensional embeddings. That motivates researchers to first project the original data into a low-

dimensional subspace, and then cluster the embedding features, using methods such as PCA, LDA [21] and sparse coding [27]. More recently, deep learning have attracted great attention in many feature learning and classification problems [13]. The advantages of deep learning lie in its composition of multiple non-linear transformations to yield more abstract and descriptive embedding representations. However, there has not been much attention paid to the potential of deep learning for unsupervised clustering problems. Moreover, generic deep architectures [13] learn all their knowledge from training data, while people’s domain expertise for specific problems are largely ignored in deep learning based approaches.

Inspired by the successful practice of sparse codes in clustering [5, 31, 26], we combine the domain expertise of sparse coding with the key ingredients of deep learning, and outline a carefully crafted deep framework for clustering. Its feature extraction layers closely mimic the process of sparse coding, using a time-unfolded structure inspired from iterative algorithms [9]. The developed feed-forward neural network, named TAG-LISTA, is specifically crafted to extract the sparse code-type features under graph constraints, that are also optimized under task-specific loss functions from end to end. Benefiting from both the sparse coding domain expertise and the large learning capacity of deep networks, the proposed model achieves notable improvements over the generic deep models of the same parameter complexity. Moreover, the learned intermediate representations continue to have clustering interpretations across different latent attributes [24]. By enforcing auxiliary clustering tasks on the hierarchy of features, we develop DTAG-LISTA and observe further performance boosts on the CMU MultiPIE dataset [10].

2. Related Work

2.1. Sparse coding for clustering

Sparse codes are proven to be an robust and efficient feature for clustering. Assuming that data samples $\mathbf{X} = [\mathbf{x}_1, \mathbf{x}_2, \dots, \mathbf{x}_n], \mathbf{x}_i \in R^{m \times 1}, i = 1, 2, \dots, n$, are encoded into their corresponding sparse codes $\mathbf{A} = [\mathbf{a}_1, \mathbf{a}_2, \dots, \mathbf{a}_n], \mathbf{a}_i \in R^{p \times 1}, i = 1, 2, \dots, n$, using a learned dictionary $\mathbf{D} = [\mathbf{d}_1, \mathbf{d}_2, \dots, \mathbf{d}_p]$, where $\mathbf{d}_i \in R^{m \times 1}, i = 1, 2, \dots, p$ are the learned atoms. The sparse

codes are obtained by solving the following convex optimization (λ is a constant):

$$\mathbf{A} = \arg \min_{\mathbf{A}} \frac{1}{2} \|\mathbf{X} - \mathbf{D}\mathbf{A}\|_F^2 + \lambda \sum_i \|\mathbf{a}_i\|_1 \quad (1)$$

In [5], the authors suggested that the sparse codes can be used to constitute the similarity graph for spectral clustering [18]. Furthermore, to capture the geometric structure of local data manifolds, the graph regularized sparse codes are further suggested in [31, 29], by solving:

$$\mathbf{A} = \arg \min_{\mathbf{A}} \frac{1}{2} \|\mathbf{X} - \mathbf{D}\mathbf{A}\|_F^2 + \lambda \sum_i \|\mathbf{a}_i\|_1 + \frac{\alpha}{2} \text{Tr}(\mathbf{A}\mathbf{L}\mathbf{A}^T) \quad (2)$$

where \mathbf{L} is the graph Laplacian matrix and can be constructed from a pre-chosen pairwise similarity matrix \mathbf{P} . More recently in [26], the authors suggested to simultaneously learn feature extraction and discriminative clustering, by formulating a task-driven sparse coding model [17]. They proved that the joint methods consistently outperformed non-joint counterparts.

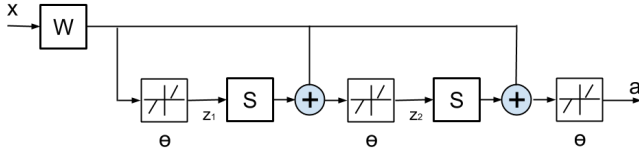


Figure 1. A LISTA network [9] with two time-unfolded stages, whose output is an approximation of the sparse code of input signal \mathbf{x} . The parameters \mathbf{W} , \mathbf{S} and θ are learned from data.

2.2. Deep learning for clustering

In [23], the authors first explored the possibility of employing deep learning in graph clustering. They first learned a nonlinear embedding of the original graph by the auto encoder (AE), and then runs K-means algorithm on the embedding to obtain clustering result. Being very straightforward, it neither exploits more adapted deep architectures nor performs any task-specific joint optimization. In [4], a deep belief network (DBN) [11] with nonparametric clustering was presented. As a generative graphical model, DBN allows for fast feature learning but is usually not as effective as AEs in learning discriminative features for clustering. In [24], the authors extended the semi non-negative matrix factorization (Semi-NMF) model [15] to a Deep Semi-NMF model, whose architecture resembles AEs.

2.3. Connecting deep learning to sparse coding

The close connection has been noticed between sparse coding and neural network. In [9], a feed-forward neural network, as illustrated in Fig. 1, is proposed to efficiently approximate the sparse code \mathbf{a} of input signal \mathbf{x} , which is obtained by solving (1) in advance. Each stage of the network updates the intermediate sparse code according to

$$\mathbf{z}_{k+1} = h_{\theta}(\mathbf{W}\mathbf{x} + \mathbf{S}\mathbf{z}_k), \quad (3)$$

where \mathbf{z}_k denotes the intermediate output of the k -th stage ($k=1, 2$), and h_{θ} is an element-wise shrinkage function:

$$[h_{\theta}(\mathbf{u})]_i = \text{sign}(\mathbf{u}_i)(|\mathbf{u}_i| - \theta_i)_+. \quad (4)$$

The network, named learned ISTA (LISTA), is a network implementation of the iterative shrinkage and thresholding algorithm (ISTA). The authors of [9] learned the network parameters \mathbf{W} , \mathbf{S} and θ as a general regression model from training data to their pre-solved sparse codes, using a back-propagation algorithm.

3. Model Formulation

The proposed pipeline consists of two blocks, and is trained end-to-end in an unsupervised way, as depicted in Fig. 2 (a). A feed-forward architecture, Task-specific And Graph-regularized LISTA (TAG-LISTA), is adopted to extract discriminative features, on top of which clustering-oriented loss functions are enforced.

3.1. TAG-LISTA: Task-specific And Graph-regularized LISTA

While LISTA is proven to be an efficient and flexible implementation of conventional sparse coding (1), it assumes the “optimal” sparse codes to be pre-obtained from (1), which implicitly requires that the dictionary \mathbf{D} is estimated [9]. In that way, LISTA could only serve as a sparse code predictor for input vectors drawn from the same distribution as the training samples, whose effectiveness further hinges on the choice of \mathbf{D} . Moreover, LISTA overlooks the useful geometric information among data points [31].

We hereby propose Task-specific And Graph-regularized LISTA (TAG-LISTA) to learn effective features for clustering, which is superior in two folds:

- TAG-LISTA learns feature optimized under clustering criteria. While LISTA merely minimize the approximation error to the optimal sparse codes on a given dataset, TAG-LISTA produces more discriminative features as well as avoids the tedious re-computation of \mathbf{A} .
- TAG-LISTA encodes the graph constraint in (2) to further regularize the solution. Previous results [31] indicate that encoding geometrical information will significantly enhance the clustering performances.

TAG-LISTA is derived from the following theorem:

Theorem 3.1. *The optimal sparse code \mathbf{A} from (2) is the fixed point of*

$$\mathbf{A} = h_{\frac{\lambda}{N}} \left[\left(\mathbf{I} - \frac{1}{N} \mathbf{D}^T \mathbf{D} \right) \cdot \mathbf{A} - \mathbf{A} \cdot \left(\frac{\alpha}{N} \mathbf{L} \right) + \frac{1}{N} \mathbf{D}^T \mathbf{X} \right], \quad (5)$$

where N is an upper bound on the largest eigenvalue of $\mathbf{D}^T \mathbf{D}$.

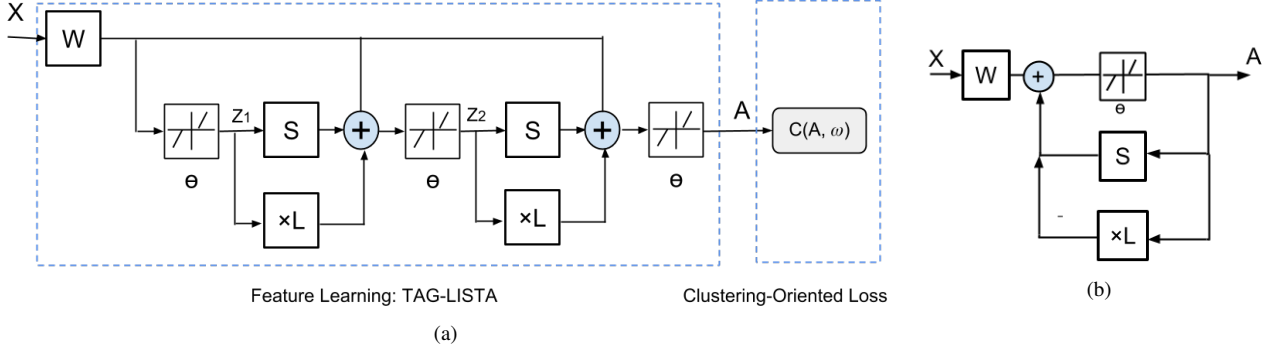


Figure 2. (a) The proposed pipeline, consisting of the TAG-LISTA network for feature learning and the clustering-oriented loss functions on its top. The parameters \mathbf{W} , \mathbf{S} , θ and ω are all learnt from training data from end to end. (b) The block diagram of solving (5).

The complete proof of Theorem 3.1 can be found in the supplementary. Theorem 3.1 outlines an iterative algorithm to solve (2). Under quite mild conditions [2], after \mathbf{A} is initialized, one may repeat the shrinkage and thresholding process in (5) until convergence. The iterative algorithm could be alternatively expressed as the block diagram in Fig. 2 (b), where

$$\mathbf{W} = \frac{1}{N} \mathbf{D}^T, \mathbf{S} = \mathbf{I} - \frac{1}{N} \mathbf{D}^T \mathbf{D}, \theta = \frac{\lambda}{N}. \quad (6)$$

In particular, we define the new operator “ $\times \mathbf{L}$ ”: $\mathbf{A} \rightarrow -\frac{\alpha}{N} \mathbf{A} \mathbf{L}$.

By time-unfolding and truncating Fig. 2 (b) to a fixed number of K iterations ($K = 2$ by default)¹, we obtain the TAG-LISTA form of the first block in Fig. 2 (a). \mathbf{W} , \mathbf{S} and θ are all to be learnt jointly from data. We are motivated from the fixed point iteration algorithm as in Fig. 2 (b), and share \mathbf{W} , \mathbf{S} and θ for both stages². Compared to the linear layers \mathbf{W} and \mathbf{S} , the activation thresholds θ are less straightforward to be updated. To facilitate training, we rewrite (4) as:

$$[h_{\theta}(\mathbf{u})]_i = \theta_i \cdot \text{sign}(\mathbf{u}_i) (|\mathbf{u}_i|/\theta_i - 1)_+ = \theta_i h_1(\mathbf{u}_i/\theta_i) \quad (7)$$

Eqn. (7) indicates that the original neuron with trainable thresholds can be decomposed into two linear scaling layers plus a unit-threshold neuron. The weights of the two scaling layers are diagonal matrices defined by θ and its element-wise reciprocal, respectively.

The graph laplacian \mathbf{L} in the new $\times \mathbf{L}$ term could be readily obtained in advance. To encode graph regularization as a prior, we fix \mathbf{L} during model training by setting its learning rate to be 0. In each stage, the $\times \mathbf{L}$ branch will execute feed-forward computation by taking the intermediate \mathbf{Z}_k ($k = 1, 2$) as its input. Its output is to be aggregated from the

¹We test larger K values (3 or 4), but they do not bring noticeable performance improvements in our clustering cases.

²Out of curiosity, we have also tried the architecture that treat \mathbf{W} , \mathbf{S} and θ in both stages as independent variables. We find that sharing parameters can significantly improve the performance.

output of the learnable \mathbf{S} layer. However, \mathbf{L} itself will not be altered by back propagations.

In sum, the graph-regularized sparse coding prior is effectively encoded in the TAG-LISTA network structure; at the same time, all the components of sparse coding can be trained jointly through back-propagation. Rather than to predict the solution of (2) exactly as in LISTA [9], the goal of TAG-LISTA is instead to learn discriminative embedding that is optimal for clustering. Therefore, the output \mathbf{A} of TAG-LISTA is not necessarily identical (or even close) to the predicted sparse codes by solving (2). By slightly abusing the notation \mathbf{A} in (2) here, we intend to remind the close analytical relationship (but not equivalence) between TAG-LISTA and (2), that makes the whole model more interpretable. It also provides us with a clue on how to effectively initialize the deep model.

3.2. Clustering-oriented loss functions

Assuming K clusters, and $\omega = [\omega_1, \dots, \omega_K]$ as the set of parameters of the loss function, where ω_i corresponds to the i -th cluster, $i = 1, 2, \dots, K$. A natural choice of the loss function is extended from the popular softmax loss in supervised learning [13], and take the entropy-like form:

$$C(\mathbf{A}, \omega) = -\sum_{i=1}^n \sum_{j=1}^K p_{ij} \log p_{ij}. \quad (8)$$

where p_{ij} denotes the the confidence probability that sample \mathbf{x}_i belongs to cluster j , $i = 1, 2, \dots, N$, $j = 1, 2, \dots, K$:

$$p_{ij} = p(j|\omega, \mathbf{a}_i) = \frac{e^{-\omega_j^T \mathbf{a}_i}}{\sum_{l=1}^K e^{-\omega_l^T \mathbf{a}_i}}, \quad (9)$$

In testing, the predicted cluster label of \mathbf{a}_i is the cluster j where it achieves the largest likelihood probability p_{ij} .

In [28], the authors proposed maximum margin clustering (MMC), which borrows the idea from the theory of SVM [6]. MMC finds a way to label the samples by running an SVM implicitly, and the SVM margin obtained would be maximized over all possible labels [30]. By referring to

the MMC definition, the authors of [26] designed the max-margin loss:

$$C(\mathbf{A}, \boldsymbol{\omega}) = \frac{\lambda}{2} \|\boldsymbol{\omega}\|^2 + \sum_{i=1}^n C(\mathbf{a}_i, \boldsymbol{\omega}). \quad (10)$$

In the above equation, the loss for an individual sample \mathbf{a}_i is defined as:

$$\begin{aligned} C(\mathbf{a}_i, \boldsymbol{\omega}) &= \max(0, 1 + f^{r_i}(\mathbf{a}_i) - f^{y_i}(\mathbf{a}_i)) \\ \text{where } y_i &= \arg \max_{j=1, \dots, K} f^j(\mathbf{a}_i) \\ r_i &= \arg \max_{j=1, \dots, K, j \neq y_i} f^j(\mathbf{a}_i). \end{aligned} \quad (11)$$

where f^j is the prototype for the j -th cluster. The predicted cluster label of \mathbf{a}_i is the cluster of the weight vector that achieves the maximum value $\boldsymbol{\omega}_j^T \mathbf{a}_i$.

3.3. Complexity and convergence

The proposed framework can handle large-scale and high-dimensional data effectively via the stochastic gradient descent (SGD) algorithm. In each step, the back propagation procedure requires only operations of order $O(p)$ [9]. The training algorithm takes $O(Cnp)$ time (C is the constant absorbing epochs, stage numbers, etc.). In addition, whereas graph regularized sparse coding (2) is hard to be parallel, SGD is easy to be parallelized.

SGD converges to stationary points under a few stricter assumptions than ones satisfied in this paper. A non-convex convergence proof assumes three times differentiable cost functions [17]. As a typical case in machine learning, we use SGD in a setting where it is not guaranteed to converge in theory, but behaves well in practice.

4. A Deeper Look: Hierarchical Clustering by DTAG-LISTA

Deep networks are renowned for their capabilities to learn semantically rich representations by hidden layers, that call for task-specific interpretations [7]. In this section, we investigate how the intermediate features \mathbf{Z}_k ($k = 1, 2$) in TAG-LISTA (see Fig. 2 (a)) can be interpreted, and further utilized to improve the model, for specific clustering tasks. Compared to related non-deep work [26], such a hierarchical clustering property is another unique advantage of being deep.

The Deep Semi-NMF model proposed in [24] presented a preliminary exploration in that way. The learnt deep model is proven to be able to learn hidden representations that grant themselves an interpretation of clustering according to different attributes. The authors considered the problem of mapping facial images to their identities. A face image also contains attributes like pose and expression that help identify the person depicted. In their experiments, the authors found that by further factorizing this mapping in

a way that each factor adds an extra layer of abstraction, the deep model could automatically learn latent intermediate representations that are implied for clustering identity-related attributes. Although there is a clustering interpretation, those hidden representations are not specifically optimized in clustering sense. Instead, the entire model is trained with only the overall reconstruction loss, after which clustering is performed using K-means on learnt features. Consequently, their clustering performance is not satisfactory, implying a large potential room for improvement.

In this work, we share the similar observation and motivation as in [24], but again in a more clustering task-specific manner. Our strategy is mainly inspired by the algorithmic framework of deeply supervised nets in [14]. As revealed in Fig. 3, the Deeply-Task-specific And Graph-regularized LISTA (**DTAG-LISTA**) brings in additional deep feedbacks, by associating a clustering-oriented local auxiliary loss $C_k(\mathbf{Z}_k, \boldsymbol{\omega}_k)$ ($k = 1, 2$) with each stage. Such an auxiliary loss takes the same form as the overall $C(\mathbf{A}, \boldsymbol{\omega})$, except that the expected cluster number may be different, depending on the auxiliary clustering task to be performed. While seeking the optimal performance of the target clustering, we also require some ‘‘satisfactory’’ level of performance on these auxiliary tasks. The DTAG-LISTA back-propagates errors not only from the overall loss layer, but also simultaneously from the auxiliary losses. As suggested in the classification experiments in [14], the auxiliary loss both acts as feature regularization to reduce generalization errors and results in faster convergence.

DTAG-LISTA explicitly targets each $C_k(\mathbf{Z}_k, \boldsymbol{\omega}_k)$ ($k = 1, 2$) at an attribute clustering task as in [24], with the difference from [24] that we perform the joint optimization altogether. In particular, DTAG-LISTA enforces a constraint at each hidden representation for directly making a good cluster prediction. In addition to the effect of the overall discriminative loss, the introduction of auxiliary losses gives another strong push for having discriminative and sensible features at each individual stage. We will also demonstrate in Section V that every \mathbf{Z}_k ($k = 1, 2$) is indeed most suited for its targeted task.

5. Experiment Results

5.1. Datasets and measurements

We evaluate the proposed model on the clustering task of three distinct datasets, including:

- **MNIST** consists of a total number of 70, 000 quasi-binary, handwritten digit images, with digits 0 to 9. The digits are normalized and centered in fixed-size images of 28×28 .
- **CMU MultiPIE** contains around 750, 000 images of 337 subjects, captured under varied laboratory condi-

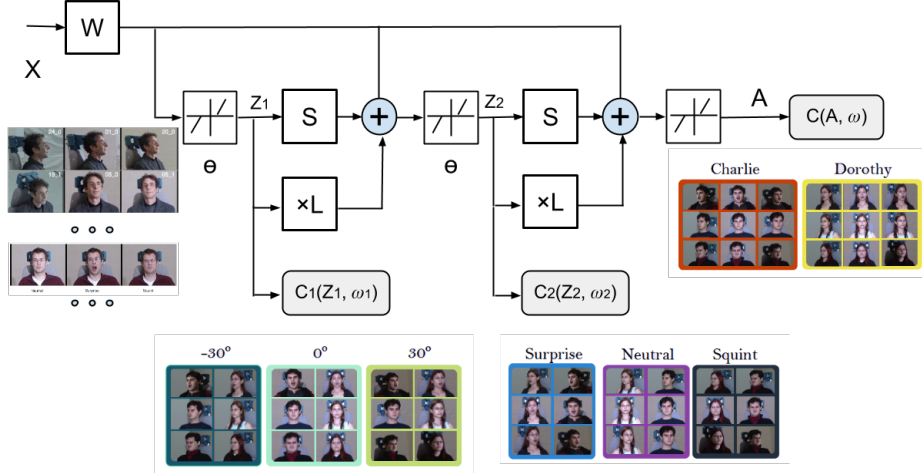


Figure 3. The DTAG-LISTA architecture, taking the CMU MultiPIE dataset for demonstration. The model is able to simultaneously learn features for pose clustering (Z_1), for expression clustering (Z_2), and for identity clustering (A). The first two attributes are related and helpful for the last (overall) task. Note that different from the example given in [24], DTAG-LISTA is also driven by two auxiliary tasks that are explicitly targeted at specific attribute clustering examples. Part of image sources are referred from [10] and [24].

tions. A unique property of CMU MultiPIE lies in that each image comes with labels for the identity, illumination, pose and expression attributes. That is why CMU MultiPIE is chosen in [24] to learn multi-attribute features (Fig. 3) for hierarchical clustering. In our experiments, we follow [24] and adopt a subset of 13, 230 images of 147 subjects in 5 different poses and 6 different emotions. Notably, we do not pre-process the images by using piece-wise affine warping as utilized by [24] to align these images.

- **COIL20** contains 1, 440 32×32 gray scale images of 20 objects (72 images per object). The images of each object were taken 5 degree apart as the object is rotated on a turntable.

We apply two widely-used measures to evaluate the performance of the clustering methods: the accuracy and the Normalized Mutual Information (NMI) [31], [5].

5.2. Experiment settings

The proposed networks are implemented using the Caffe package [12]. The network takes $K = 2$ stages by default. We use a constant learning rate of 0.01 with no momentum, and a batch size of 128. The clipping is performed [20] on the gradients with a threshold of 1. For the graph regularization. Experiments run on a workstation with 12 Intel Xeon 2.67GHz CPUs and 1 GTX680 GPU. The training takes approximately 1 hour on the MNIST dataset. It is also observed that the training efficiency of our model scales approximately linearly with data.

An appealing highlight of (D)TAG-LISTA lies in its

very effective and straightforward initialization strategy. While many neural networks train well with random initializations without pre-training, given the training data is sufficient, it has been discovered that poorly initialized networks has hampered the effectiveness of first-order methods (e.g., SGD) in certain cases [22]. For (D)TAG-LISTA, it is however much easier to initialize the model in the right regime, benefiting from the **analytical relationships between sparse coding and network hyperparameters** defined in (6). That is especially meaningful when clustering on relatively small-scale datasets, e.g., COIL 20.

In our experiments, we set the default value of α to be 5, p to be 128, and λ to be chosen from [0.1, 1] by cross-validation. A dictionary D is first learned from X by K-SVD [1]. W , S and θ are then initialized based on (6). L is also pre-calculated from P , which is formulated by the Gaussian Kernel: $P_{ij} = \exp(-\frac{\|x_i - x_j\|_2^2}{\delta^2})$ (δ is also selected by cross-validation). After obtaining the output A from the initial (D)TAG-LISTA models, ω (or ω_k) could be initialized based on minimizing (8) or (10) over A (or Z_k).

5.3. Comparison experiments and analysis

5.3.1 Benefits of the task-specific deep architecture

We denote the proposed model of TAG-LISTA plus entropy-minimization loss (EML) (8) as TAG-LISTA-EML, and the one plus maximum-margin loss (MML) (10) as TAG-LISTA-MML, respectively. We refer to the initializations of the proposed joint models as their “non-joint” counterparts, NJ-TAG-LISTA-EML and NJ-TAG-LISTA-MML (NJ short for non-joint), respectively.

To verify the important argument that *the proposed*

model benefits from the task-specific TAG-LISTA architecture, rather than just the large learning capacity of generic deep models, we design a **Baseline Encoder** (BE) for comparison, which is a fully-connected feedforward network, consisting of three hidden layers of dimension p with ReLU neurons. It is obvious that the baseline encoder thus has the *same parameter capacity* as TAG-LISTA³. The BEs are also tuned by EML or MML in the same way, denoted as BE-EML or BE-MML, respectively.

Moreover, we compare the proposed models with their closest “shallow” competitors, i.e., the joint optimization methods of graph-regularized sparse coding and discriminative clustering described in [26]. We re-implement their work using both (8) or (10) losses, denoted as SC-EML and SC-MML (SC short for sparse coding). Since in [26] the authors already revealed SC-MML outperforms the classical methods such as MMC and ℓ_1 graph methods, we do not compare with them again. In addition, we also include Deep Semi-NMF [24] as one state-of-the-art deep learning-based clustering work.⁴

As revealed by the full comparison results in Table 1, the proposed task-specific deep architectures outperform other with noticeable margins, partially owing to the underlying domain expertise that guides the data-driven training in a more principled way. In contrast, the “general-architecture” baseline encoders (BE-EML and BE-MML), which have the same parameter complexity, appear to produce much worse (even worst) results. On the other hand, it is evident that the proposed end-to-end optimized models each outperform their “non-joint” fellows. For example, on the MNIST dataset, TAG-LISTA-MML surpasses NJ-TAG-LISTA-MML by around 4% in accuracy and 5% in NMI.

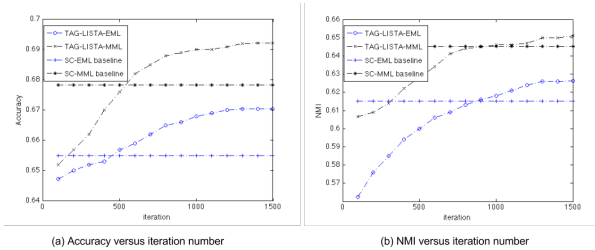


Figure 4. The accuracy and NMI measurement plots of TAG-LISTA-EML/TAG-LISTA-MML on the MNIST dataset, starting from the initialization, and tested every 100 iterations. The accuracy and NMI of SC-EML/SC-MML are also plotted as baseline references.

When comparing the TAG-LISTA-EML/TAG-LISTA-MML with SC-EML/SC-MML, we draw the convincing

³except for the “ θ ” layers, each of which contains only p free parameters and thus ignored

⁴we compare our results with their reported performance numbers on CMU MultiPIE. With various component numbers tested in [24], we choose the best results (60 components).

conclusion, that adopting a more parameterized deep architecture allows for a larger feature learning capacity compared to conventional sparse coding. Although similar points are well made in many other fields [13], we are interested in a closer look between the two. Fig. 4 plots the clustering accuracy and NMI curves of TAG-LISTA-EML/TAG-LISTA-MML on the MNIST dataset, along with iteration numbers. Each model is well initialized at the very beginning, and the clustering accuracy and NMI are computed every 100 iterations. At first, the clustering performances of deep models are even slightly worse than sparse-coding methods, mainly since the initialization of TAG-LISTA hinges on a truncated approximated of graph-regularized sparse coding. After a small number of iterations, the performance of each model surpasses sparse coding very soon, and continue rising monotonically until reaching a higher plateau.

5.3.2 Effects of graph regularization

In (2), the graph regularization term imposes stronger smoothness constraints on the sparse codes with larger α , and the same way in TAG-LISTA. We investigate how the clustering performances of TAG-LISTA-EML/TAG-LISTA-MML are influenced by various α values. From Fig. 5, 6 and 7, we observe the identical general tendency on all three datasets, that while α increases, the accuracy/NMI result will first rise then decrease, with the peak appearing between $\alpha \in [5, 10]$ (thus we choose $\alpha = 5$ as the default value). As an interpretation, the local manifold information is not sufficiently encoded when α is too small ($\alpha = 0$ will completely disable the $\times L$ branch of TAG-LISTA). On the other hand, when α turns overly large, the sparse codes are “over-smoothened” with a reduced discriminative ability. Note similar phenomena are also reported in other relevant literature, e. g. , [31, 26].

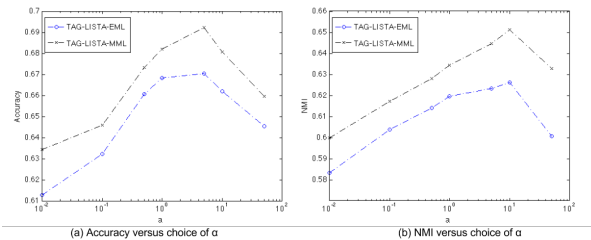


Figure 5. The clustering accuracy and NMI measurement plots (x-axis logarithm scale) of TAG-LISTA-EML/TAG-LISTA-MML versus the parameter choices of α , on the MNIST dataset .

On the other hand, comparing among Fig. 5, 6 and 7, it is noteworthy to observe how graph regularization behaves differently on three of them. We notice that the COIL20 dataset is most sensitive to the choice of α , and increasing α from 0.01 to 50 leads to an improvement of more than

Table 1. Accuracy and NMI performance comparisons on all three datasets

		TAG-LISTA -EML	TAG-LISTA -MML	NJ-TAG-LISTA -EML	NJ-TAG-LISTA -MML	BE -EML	BE -MML	SC -EML	SC -MML	Deep Semi-NMF
<i>MNIST</i>	Acc	0.6704	0.6922	0.6472	0.5052	0.5401	0.6521	0.6550	0.6784	/
	NMI	0.6261	0.6511	0.5624	0.6067	0.5002	0.5011	0.6150	0.6451	/
<i>CMU MultiPIE</i>	Acc	0.2176	0.2347	0.1727	0.1861	0.1204	0.1451	0.2002	0.2090	0.17
	NMI	0.4338	0.4555	0.3167	0.3284	0.2672	0.2821	0.3337	0.3521	0.36
<i>COIL20</i>	Acc	0.8553	0.8991	0.7432	0.7882	0.7441	0.7645	0.8225	0.8658	/
	NMI	0.9090	0.9277	0.8707	0.8814	0.8028	0.8321	0.8850	0.9127	/

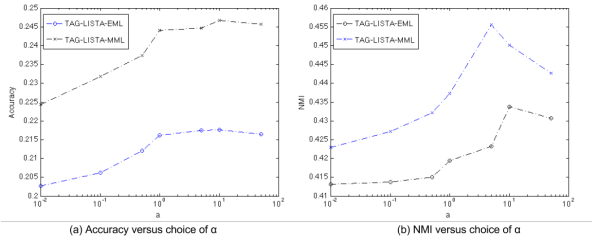


Figure 6. The clustering accuracy and NMI measurement plots (x-axis logarithm scale) of TAG-LISTA-EML/TAG-LISTA-MML versus the parameter choices of α , on the CMU MultiPIE dataset.

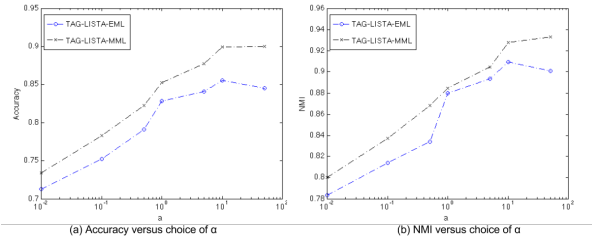


Figure 7. The clustering accuracy and NMI measurement plots (x-axis logarithm scale) of TAG-LISTA-EML/TAG-LISTA-MML versus the parameter choices of α , on the COIL20 dataset.

10%, in terms of both accuracy and NMI, for both TAG-LISTA-EML and TAG-LISTA-MML. It verifies the significance of graph regularization when applied to small-scale, high-dimensional datasets [29]. On the MNIST dataset, both models obtain a gain of up to 6% in accuracy and 5% in NMI, by tuning α from 0.01 to 10. However, unlike COIL20 that almost always favors larger α , the model performance on the MNIST dataset tends to be not only saturated, but even significantly hampered when α continues rising to 50. The CMU MultiPIE dataset witnesses moderate improvements of around 2% in both measurements. It seems not as sensitive to α in our experiments, potentially due to the complex variability in original images that makes the graph W unreliable for estimating the underlying manifold geometry. We suspect that more sophisticated graphs may help alleviate the problem, and will explore it in future.

5.3.3 Scalability and robustness

On the MNIST dataset, We re-conduct the clustering experiments with the cluster number N_c ranging from 2 to 10,

using TAG-LISTA-EML/TAG-LISTA-MML. For each N_c except for 10, 10 test runs are conducted on different randomly chosen clusters, and the final scores are obtained by averaging over the tests. Fig. 8 shows the clustering accuracy and NMI measurements versus the number of clusters. The clustering performance transits smoothly and robustly when the task scale changes.

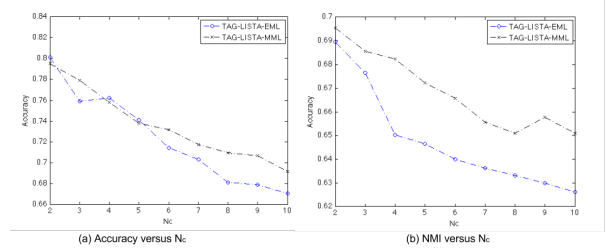


Figure 8. The clustering accuracy and NMI measurement plots of TAG-LISTA-EML/TAG-LISTA-EML versus the cluster number N_c ranging from 2 to 10, on the MNIST dataset.

To examine the proposed models' robustness to noise, we add various Gaussian noise, whose standard deviation s ranges from 0 (noiseless) to 0.3, to the MNIST data, and then re-train our model. Fig. 9 indicates that both TAG-LISTA-EML and TAG-LISTA-MML own certain robustness to noise. When s is less than 0.1, there is even little visible performance degradation. While TAG-LISTA-MML constantly outperforms TAG-LISTA-EML in all our experiments (as MMC is well-known to be highly discriminative [28]), it is interesting to observe in Fig. 9 that the latter is slightly more robust to noise than the former, perhaps because the probability-driven loss form (8) of EML allows for more flexibility.

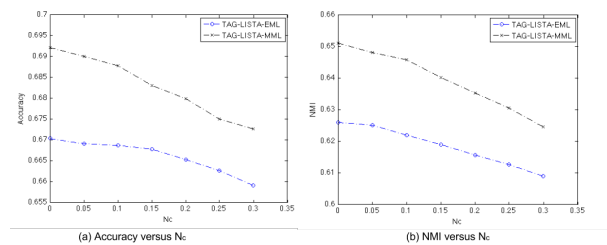


Figure 9. The clustering accuracy and NMI measurement plots of TAG-LISTA-EML/TAG-LISTA-MML versus the noise level s , on the MNIST dataset.

5.4. Hierarchical clustering on CMU MultiPIE

As observed, CMU MultiPIE remains very challenging for the basic identity clustering task. However, it comes with several other attributes: pose, expression, and illumination, which could be of assistance in our proposed DTAG-LISTA framework. In this section, we adopt the similar setting suggested in [24] applied on the same CMU MultiPIE subset, setting pose clustering as the Stage I auxiliary task, and expression clustering as the Stage II auxiliary task⁵. In that way, we target $C_1(\mathbf{Z}_1, \omega_1)$ at 5 clusters, $C_2(\mathbf{Z}_2, \omega_2)$ at 6 clusters, and finally $C(\mathbf{A}, \omega)$ as 147 clusters.

The training of DTAG-LISTA-EML/DTAG-LISTA-MML follows the same above process except for considering extra back-propagated gradients from task $C_k(\mathbf{Z}_k, \omega_k)$ in Stage k ($k = 1, 2$). After then, we test each $C_k(\mathbf{Z}_k, \omega_k)$ separately on their targeted task. Since in DTAG-LISTA, each auxiliary task is also jointly optimized with its input intermediate feature \mathbf{Z}_k , which differentiate our methodology substantially from [24], there is no surprise to see in Table 2 that each auxiliary task obtains much improved performances than [24]⁶. Most notably, the performances of the overall identity clustering task witness a **very impressive boost of around 7% in accuracy**. We also test DTAG-LISTA-EML/DTAG-LISTA-MML with only $C_1(\mathbf{Z}_1, \omega_1)$ or $C_2(\mathbf{Z}_2, \omega_2)$ kept. Experiments verify that by adding auxiliary tasks gradually, the overall task keeps being benefited. Those auxiliary tasks, when enforced together, can also reinforce each other mutually.

Table 2. Effects of incorporating auxiliary clustering tasks in DTAG-LISTA-EML/DTAG-LISTA-MML

Method	Stage I		Stage II		confusion	
	Task	Acc	Task	Acc	Task	Acc
DTAG-LISTA-EML	/	/	/	/	Identity	0.2176
	Pose	0.5067	/	/	Identity	0.2303
	/	/	Expression	0.3676	Identity	0.2507
	Pose	0.5407	Expression	0.4027	Identity	0.2833
DTAG-LISTA-MML	/	/	/	/	Identity	0.2347
	Pose	0.5251	/	/	Identity	0.2635
	/	/	Expression	0.3988	Identity	0.2858
	Pose	0.5538	Expression	0.4231	Identity	0.3021

One might be curious that, **which one matters more in the performance boost**: the deeply task-specific architecture that brings extra discriminative feature learning, or the proper design of auxiliary tasks that capture the intrinsic data structure characterized by attributes?

To answer this important question, we vary the target cluster number in either $C_1(\mathbf{Z}_1, \omega_1)$ or $C_2(\mathbf{Z}_2, \omega_2)$, and re-

⁵In fact, although claimed to be applicable to multiple attributes, [24] only examined the first level features for pose clustering without considering expressions, since it relied on a warping technique to pre-process images, that gets rid of most expression variability.

⁶In [24] Table. 2, it reports that the best accuracy of pose clustering task falls around 28%, using the most suited layer features.

conduct the experiments. Table 3 reveals that more auxiliary tasks, even those without explicit task-specific interpretations (e.g., partitioning the Multi-PIE subset into 4, 8, 12 or 20 clusters hardly makes semantic sense), may still help gain better performances. They simply promote more discriminative feature learning in a low-to-high, coarse-to-fine scheme. In fact, it is a complementary observation to the conclusion found in classification [14]. On the other hand, while the target cluster numbers of auxiliary tasks get closer to the ground-truth (5 and 6 here), the models achieve better performances. When properly “matched”, every hidden representation in each layer is in fact most suited for clustering the attributes corresponding to the layer of interest. The whole model then resembles the problem of sharing low-level feature filters among several relevant high-level tasks in convolutional networks [8], but in a distinct context.

Table 3. Effects of varying target cluster numbers of auxiliary tasks in DTAG-LISTA-EML/DTAG-LISTA-MML

Method	#clusters in Stage I	#clusters in Stage II	Overall Accuracy
DTAG-LISTA-EML	4	4	0.2827
	8	8	0.2813
	12	12	0.2802
	20	20	0.2757
DTAG-LISTA-MML	4	4	0.3030
	8	8	0.3006
	12	12	0.2927
	20	20	0.2805

The conclusion is hence that, the deeply-supervised fashion tends to be useful for the proposed deep clustering models, even when there are no extra attributes explicitly available to construct a practically meaningful hierarchical clustering problem. However, it is encouraged to exploit those attributes when available, as they lead to not only superior performances but more clearly interpretable models. The learned intermediate features can be potentially utilized for multi-task learning [25].

6. Conclusion

In this paper, we present a deep learning-based clustering framework. Trained from end to end, it features a task-specific deep architecture inspired by the sparse coding domain expertise, which is optimized under clustering-oriented losses. Such a well-crafted architecture leads to more effective initialization and training, and significantly outperforms generic architectures of the same parameter capacity. The model could be further interpreted and enhanced, by introducing auxiliary clustering losses to the intermediate features. Extensive experiments verify the effectiveness and robustness of the proposed model.

References

- [1] M. Aharon, M. Elad, and A. Bruckstein. K-svd: An algorithm for designing overcomplete dictionaries for sparse representation. *Signal Processing, IEEE Transactions on*, 54(11):4311–4322, 2006. **5**
- [2] A. Beck and M. Teboulle. A fast iterative shrinkage-thresholding algorithm for linear inverse problems. *SIAM Journal on Imaging Sciences*, 2(1):183–202, 2009. **3**
- [3] C. Biernacki, G. Celeux, and G. Govaert. Assessing a mixture model for clustering with the integrated completed likelihood. *Pattern Analysis and Machine Intelligence, IEEE Transactions on*, 22(7):719–725, 2000. **1**
- [4] G. Chen. Deep learning with nonparametric clustering. *arXiv preprint arXiv:1501.03084*, 2015. **2**
- [5] B. Cheng, J. Yang, S. Yan, Y. Fu, and T. S. Huang. Learning with l1 graph for image analysis. *Image Processing, IEEE Transactions on*, 19(4):858–866, 2010. **1, 2, 5**
- [6] C. Cortes and V. Vapnik. Support-vector networks. *Machine learning*, 20(3):273–297, 1995. **3**
- [7] J. Donahue, Y. Jia, O. Vinyals, J. Hoffman, N. Zhang, E. Tzeng, and T. Darrell. Decaf: A deep convolutional activation feature for generic visual recognition. *arXiv preprint arXiv:1310.1531*, 2013. **4**
- [8] X. Glorot, A. Bordes, and Y. Bengio. Domain adaptation for large-scale sentiment classification: A deep learning approach. In *International Conference on Machine Learning (ICML)*, pages 513–520, 2011. **8**
- [9] K. Gregor and Y. LeCun. Learning fast approximations of sparse coding. In *International Conference on Machine Learning (ICML)*, pages 399–406, 2010. **1, 2, 3, 4**
- [10] R. Gross, I. Matthews, J. Cohn, T. Kanade, and S. Baker. Multi-pie. *Image and Vision Computing*, 28(5):807–813, 2010. **1, 5**
- [11] G. Hinton, S. Osindero, and Y.-W. Teh. A fast learning algorithm for deep belief nets. *Neural computation*, 18:1527–1554, 2006. **2**
- [12] Y. Jia, E. Shelhamer, J. Donahue, S. Karayev, J. Long, R. Girshick, S. Guadarrama, and T. Darrell. Caffe: Convolutional architecture for fast feature embedding. In *Proceedings of the ACM International Conference on Multimedia*, pages 675–678. ACM, 2014. **5**
- [13] A. Krizhevsky, I. Sutskever, and G. E. Hinton. Imagenet classification with deep convolutional neural networks. In *Advances in Neural Information Processing Systems (NIPS)*, pages 1097–1105, 2012. **1, 3, 6**
- [14] C.-Y. Lee, S. Xie, P. Gallagher, Z. Zhang, and Z. Tu. Deeply-supervised nets. *arXiv preprint arXiv:1409.5185*, 2014. **4, 8**
- [15] T. Li and C. Ding. The relationships among various nonnegative matrix factorization methods for clustering. In *Data Mining, 2006. ICDM'06. Sixth International Conference on*, pages 362–371. IEEE, 2006. **2**
- [16] X. Li, K. Zhang, and T. Jiang. Minimum entropy clustering and applications to gene expression analysis. In *Computational Systems Bioinformatics Conference (CSB)*, pages 142–151. IEEE, 2004. **1**
- [17] J. Mairal, F. Bach, and J. Ponce. Task-driven dictionary learning. *Pattern Analysis and Machine Intelligence, IEEE Transactions on*, 34(4):791–804, 2012. **2, 4**
- [18] A. Y. Ng, M. I. Jordan, Y. Weiss, et al. On spectral clustering: Analysis and an algorithm. *Advances in Neural Information Processing Systems (NIPS)*, 2:849–856, 2002. **2**
- [19] F. Nie, D. Xu, I. W. Tsang, and C. Zhang. Spectral embedded clustering. In *International Joint Conference on Artificial Intelligence (IJCAI)*, pages 1181–1186, 2009. **1**
- [20] R. Pascanu, T. Mikolov, and Y. Bengio. On the difficulty of training recurrent neural networks. In *International Conference on Machine Learning (ICML)*, pages 1310–1318, 2013. **5**
- [21] V. Roth and T. Lange. Feature selection in clustering problems. In *Advances in Neural Information Processing Systems (NIPS)*, 2003. **1**
- [22] I. Sutskever, J. Martens, G. Dahl, and G. Hinton. On the importance of initialization and momentum in deep learning. In *International Conference on Machine Learning (ICML)*, pages 1139–1147, 2013. **5**
- [23] F. Tian, B. Gao, Q. Cui, E. Chen, and T.-Y. Liu. Learning deep representations for graph clustering. In *Twenty-Eighth AAAI Conference on Artificial Intelligence*, 2014. **2**
- [24] G. Trigeorgis, K. Bousmalis, S. Zafeiriou, and B. Schuller. A deep semi-nmf model for learning hidden representations. In *International Conference on Machine Learning (ICML)*, pages 1692–1700, 2014. **1, 2, 4, 5, 6, 8**
- [25] Y. Wang, D. Wipf, Q. Ling, W. Chen, and I. Wassail. Multi-task learning for subspace segmentation. In *International Conference on Machine Learning (ICML)*, 2015. **8**
- [26] Z. Wang, Y. Yang, S. Chang, J. Li, S. Fong, and T. S. Huang. A joint optimization framework of sparse coding and discriminative clustering. In *International Joint Conference on Artificial Intelligence (IJCAI)*, 2015. **1, 2, 4, 6**
- [27] J. Wright, A. Y. Yang, A. Ganesh, S. S. Sastry, and Y. Ma. Robust face recognition via sparse representation. *Pattern Analysis and Machine Intelligence, IEEE Transactions on*, 31(2):210–227, 2009. **1**
- [28] L. Xu, J. Neufeld, B. Larson, and D. Schuurmans. Maximum margin clustering. In *Advances in Neural Information Processing Systems (NIPS)*, pages 1537–1544, 2004. **1, 3, 7**
- [29] Y. Yang, Z. Wang, J. Yang, J. Wang, S. Chang, and T. S. Huang. Data clustering by laplacian regularized l1-graph. In *Twenty-Eighth AAAI Conference on Artificial Intelligence*, 2014. **2, 7**
- [30] B. Zhao, F. Wang, and C. Zhang. Efficient maximum margin clustering via cutting plane algorithm. In *SIAM International Conference on Data Mining (SDM)*, pages 751–762, 2008. **3**
- [31] M. Zheng, J. Bu, C. Chen, C. Wang, L. Zhang, G. Qiu, and D. Cai. Graph regularized sparse coding for image representation. *Image Processing, IEEE Transactions on*, 20(5):1327–1336, 2011. **1, 2, 5, 6**